Asian Journal of Current Research in Clinical Cancer
ISSN: 3062-4444
2022, Volume 2, Issue 1, Page No: 47-59

Available online at: www.galaxypub.co/page/journals

Galaxy Publication

Galaxy Publication

Metabolomic Signatures of Radical Hemithoracic Radiotherapy Associate with Survival in Malignant Pleural Mesothelioma

M. Opiyo[1*], A. Wanjiku[1], B. Kamau[1]

[1]Department of Medical Oncology, Faculty of Health Sciences, University of Nairobi, Nairobi, Kenya.

***E-mail** ✉ nairobi.medonc.13@outlook.com

Received: 23 October 2021; **Revised:** 27 January 2022; **Accepted:** 03 February 2022

ABSTRACT

Radical hemithoracic radiotherapy (RHRT) offers a promising approach to extend survival in patients with malignant pleural mesothelioma. In this study, we examined how RHRT influences the systemic metabolic profile and whether these changes correlate with clinical outcomes. Nineteen patients underwent RHRT at 50 Gy delivered over 25 fractions. Serum metabolite levels were analyzed before and after treatment using targeted liquid chromatography-tandem mass spectrometry. Statistical modeling, including OPLS-DA and PLS regression, was used to identify treatment-induced metabolomic shifts and their relationship with overall survival. RHRT was associated with marked reductions in multiple metabolite classes, including citrulline and taurine, C14, C18:1, and C18:2 acyl-carnitines, and several unsaturated long-chain phosphatidylcholines (PC ae 42:5, PC ae 44:5, PC ae 44:6). Pathway analysis indicated that arginine metabolism and polyamine synthesis were the most affected. Notably, alterations in amino acids and acyl-carnitines explained approximately 60% of the variability in overall survival among patients. These results suggest that RHRT exerts profound systemic metabolic effects, some of which may serve as predictive biomarkers. Incorporating metabolomic profiling into the clinical management of malignant pleural mesothelioma may enhance patient stratification and guide personalized treatment decisions.

Keywords: Metabolomics, Mesothelioma, Radiotherapy, Biomarkers, Personalized medicine

How to Cite This Article: Opiyo M, Wanjiku A, Kamau B. Metabolomic Signatures of Radical Hemithoracic Radiotherapy Associate with Survival in Malignant Pleural Mesothelioma. Asian J Curr Res Clin Cancer. 2022;2(1):47-59. https://doi.org/10.51847/kpSHBH3R89

Introduction

Malignant pleural mesothelioma (MPM) is a rare and aggressive malignancy originating from the pleura, with a strong etiological link to asbestos exposure [1]. Due to its long latency period, invasive growth, and aggressive clinical behavior, MPM is often diagnosed at an advanced stage and carries a poor prognosis, with untreated patients typically surviving less than one year [2]. Current standard-of-care for non-metastatic MPM relies on a trimodal approach that integrates surgery, chemotherapy, and sequential radiotherapy (RT) [3, 4]. Over recent decades, RT technology has advanced considerably [5], with intensity-modulated radiation therapy (IMRT) emerging as a prominent method that allows highly conformal dosing across the hemithorax while minimizing exposure to surrounding healthy tissues. In the context of MPM, this technique—referred to as radical hemithoracic radiotherapy (RHRT)—is delivered with curative intent. Despite its potential therapeutic benefit, the broad clinical implementation of RHRT remains cautious due to concerns regarding toxicity [6], although recent studies have demonstrated promising survival outcomes with manageable adverse effects [7–9].

Nevertheless, patient responses to RHRT remain heterogeneous, highlighting the urgent need for prognostic biomarkers to guide personalized treatment. Understanding the molecular and systemic effects of RHRT is essential for identifying patients most likely to benefit. In this regard, metabolomics—the comprehensive study of small-molecule metabolites (<1 kDa) in biological samples—offers a powerful approach to monitor biochemical changes resulting from both physiological and pathological processes, as well as interventions such as RT [10–12]. Alterations in serum metabolites may serve as potential biomarkers reflecting whole-body responses to therapy. While metabolomics has been extensively applied to study systemic effects of anticancer

drugs across multiple tumor types [13–16], few studies have investigated RT-induced metabolic changes, and none specifically in MPM [17–23].

To address this gap, the present study aimed to explore the systemic metabolic effects of RHRT in MPM patients by analyzing serum metabolite profiles before and after treatment. This translational investigation provides insights into biochemical alterations induced by RHRT and evaluates their potential association with clinical outcomes, particularly focusing on amino acid and lipid metabolism pathways relevant to treatment efficacy.

Results and Discussion

Baseline clinical and demographic characteristics

The study cohort comprised 19 patients with non-metastatic MPM who underwent RHRT at a total dose of 50 Gy in 25 fractions, with a simultaneous integrated boost of 60 Gy to residual active tumor. Patient demographics and clinical characteristics are summarized in **Table 1**. The median age was 70 years (range: 33–79), and males predominated (89%). At baseline, 31% of patients had an ECOG performance status (PS) of 0, 53% had a PS of 1, and 16% had a PS of 2. Most tumors were epithelioid (95%), with the remaining 5% showing biphasic histology. Disease stage was evenly distributed, with 47% classified as stage I–II and 53% as stage III–IV. Prior surgical interventions included diagnostic biopsy (63%), lung-sparing pleurectomy/decortication (26%), and decortication (11%), leaving macroscopic residual disease. All patients received systemic chemotherapy with pemetrexed and cisplatin prior to RHRT, which was initiated 4–6 weeks following the chemotherapy regimen.

Table 1. Clinical characteristics of 19 malignant pleural mesothelioma (MPM) patients.

Characteristics	n (%)
Age (years), median, range	70 (33–79)
Sex	
Female	2 (11%)
Male	17 (89%)
Performance Status *	
0	6 (31%)
1	10 (53%)
2	3 (16%)
Histology	
Epithelioid	18 (95%)
Nonepithelioid	1 (5%)
Stage	
I–II	9 (47%)
III–IV	10 (53%)
Chemotherapy	
Pemetrexed, cisplatin	19 (100%)
Surgery	
Pleurectomy/decortication (P/D)	5 (26%)
Decortication	2 (11%)
Biopsy	12 (63%)

* Evaluated by ECOG, Eastern Cooperative Oncology Group.

The reference cohort comprised 15 MPM patients who received conventional palliative local radiotherapy (LRT). This group was largely comparable to the RHRT cohort in terms of demographic and clinical features, and patients similarly underwent lung-sparing surgery and systemic chemotherapy.

Impact of RHRT on the serum metabolome

To explore the systemic biochemical effects of RHRT, we analyzed serum metabolomic profiles before and after treatment. A targeted panel of 188 metabolites spanning multiple metabolic pathways was measured. Metabolites

with concentrations below the limit of detection (n = 27) were excluded from subsequent analyses. Initial exploratory analysis using principal component analysis (PCA) revealed no outliers, and baseline versus post-RHRT samples appeared homogeneous, without distinct clustering related to patient subgroups or interventions. However, PCA captured only 22% of the total variance between baseline and post-RHRT samples, highlighting the need for a supervised approach.

Orthogonal partial least squares discriminant analysis (OPLS-DA) effectively distinguished the pre- and post-RHRT serum metabolomic profiles, demonstrating significant discriminatory power (**(Figure 1a)**; p = 0.007, CV-ANOVA). The model performed robustly under leave-one-out cross-validation (LOOCV), with $R^2 = 0.77$ and $Q^2 = 0.54$, and permutation testing confirmed minimal risk of overfitting **(Figure 1b)**. To quantify RHRT-induced metabolic perturbations, the relative percent change (Δ%) was calculated for metabolites with VIP > 1 that contributed most to the OPLS-DA model **(Figure 1c)**. Following RHRT, 52% of the analyzed metabolites exhibited changes of ≥10%, with 14 metabolites upregulated and 69 downregulated. Importantly, these alterations were not correlated with the presence of gross residual disease, suggesting that they primarily reflect host systemic metabolic responses rather than tumor burden.

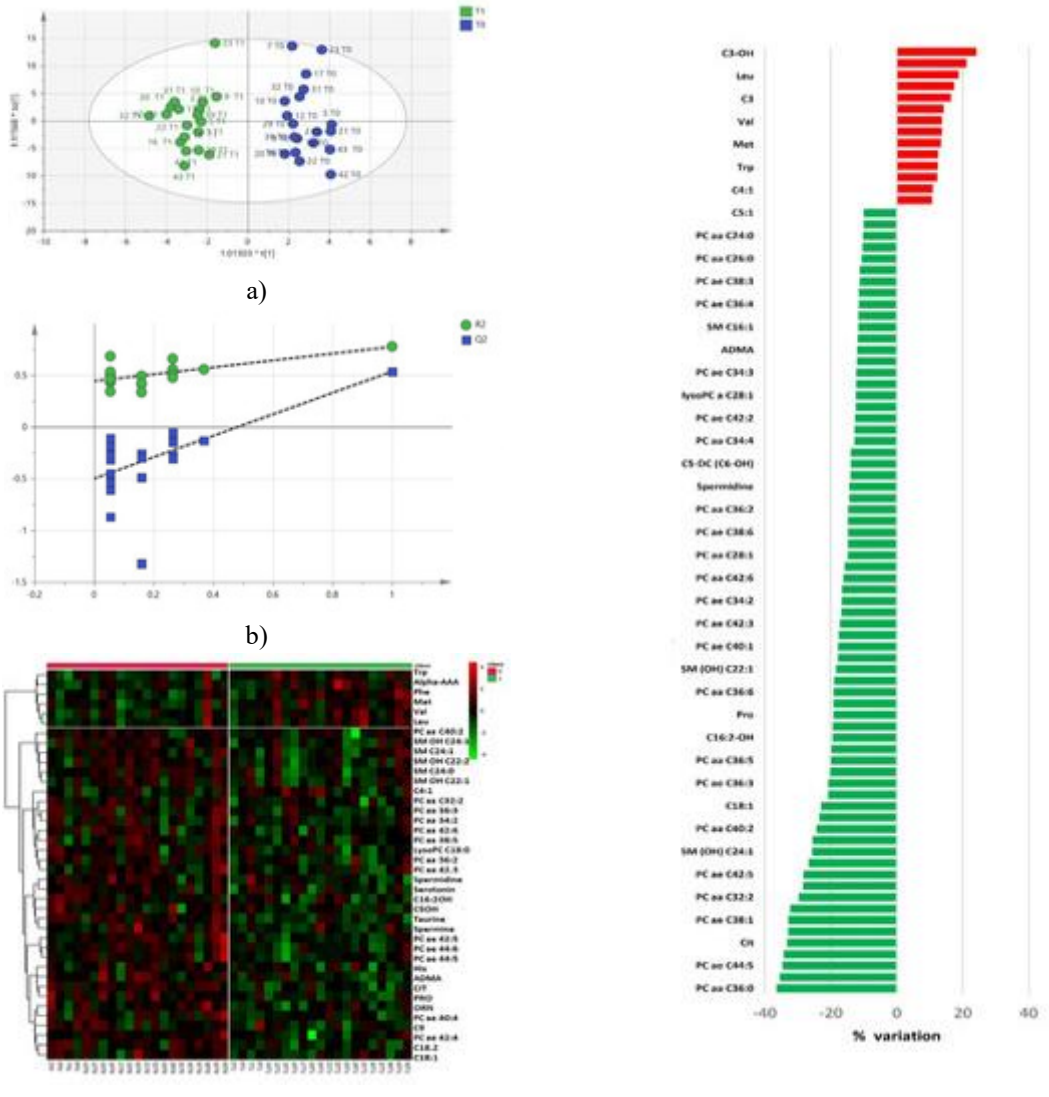

Figure 1. Systemic Metabolic Effects of RHRT in MPM Patients

Orthogonal partial least squares discriminant analysis (OPLS-DA) distinguished serum metabolomic profiles of patients prior to (T0, blue) and following (T1, green) radical hemithoracic radiotherapy (RHRT) **(Figure 1a)**. Permutation testing validated the model, showing that R^2 and Q^2 values from randomized models were

substantially lower than the original, confirming the robustness of the discrimination **(Figure 1b)**. The relative changes in metabolite concentrations contributing most to the model (VIP > 1) are presented in **Figure 1c**, while a heat map illustrates metabolites that significantly increased (red) or decreased (green) post-treatment, with color intensity corresponding to the magnitude of change **(Figure 1d)**.

Overall, RHRT was associated with a widespread reduction in serum metabolite levels. Only a limited subset, primarily amino acids, showed elevated levels after treatment, including phenylalanine, tryptophan, valine, leucine, alpha-aminoadipic acid, methionine, and carnitine. Conversely, most phospholipid species, including phosphatidylcholines (PC), lysophosphatidylcholines (lysoPC), and sphingomyelins (SM), exhibited marked decreases. The largest changes were observed for citrulline ($p = 9 \times 10^{-6}$, $q = 0.001$) and taurine ($p = 3 \times 10^{-5}$, $q = 0.002$) among amino acids, and for acyl-carnitines C14, C18:1, and C18:2 (p-values ranging $2.8 \times 10^{-4} – 0.002$). Among phospholipids, PC ae C42:5, C44:5, and C44:6 were significantly reduced ($p \leq 0.001$). Examination of individual patient data confirmed a consistent pattern of metabolite reduction across the cohort, indicating a systemic metabolic response to RHRT rather than effects driven by residual tumor burden.

Table 2. Metabolites significantly altered as effect of radical hemithoracic radiotherapy (RHRT) in 19 MPM patients.

Class	Name	Mean (µM) ± SD		Fold Change	Trend	p-Value	q-Value
		Baseline	Post-HRT				
Amino acids and derivatives	Cit	33.22 ± 7.02	22.19 ± 7.15	0.67	↓	9.0×10^{-6}	0.001
	ADMA	0.57 ± 0.06	0.5 ± 0.09	0.88	↓	0.007	0.085
	Orn	71.74 ± 9.56	62.89 ± 13.15	0.88	↓	0.017	0.113
	Pro	220.95 ± 36.99	178.47 ± 63.76	0.81	↓	0.005	0.078
	Putrescine	0.14 ± 0.03	0.13 ± 0.04	0.89	↓	0.027	0.149
	Serotonin	0.48 ± 0.22	0.36 ± 0.22	0.75	↓	0.005	0.078
	Spermidine	0.13 ± 0.03	0.11 ± 0.03	0.86	↓	0.010	0.099
	Spermine	0.19 ± 0.01	0.18 ± 0.01	0.96	↓	0.016	0.113
	Taurine	104.05 ± 18.69	74.49 ± 22.79	0.72	↓	3.0×10^{-5}	0.002
	total DMA	1.06 ± 0.31	0.94 ± 0.34	0.88	↓	0.024	0.139
	Phe	70.96 ± 11.05	79.71 ± 8.17	1.14	↑	0.009	0.095
	Val	178.21 ± 38.35	202.63 ± 36.56	1.12	↑	0.035	0.176
	alpha-AAA	1.17 ± 0.58	1.42 ± 0.34	1.21	↑	0.035	0.176
	Trp	46.96 ± 9.37	52.78 ± 10.89	1.12	↑	0.039	0.176
Acyl-carnitines	C10:2	0.08 ± 0.01	0.06 ± 0.04	0.73	↓	0.012	0.104
	C14	0.06 ± 0.02	0.04 ± 0.02	0.79	↓	0.002	0.038
	C14:1-OH	0.02 ± 0.01	0.02 ± 0.01	0.83	↓	0.032	0.174
	C:16	0.15 ± 0.03	0.12 ± 0.05	0.81	↓	0.012	0.104
	C16:2-OH	0.01 ± 0.005	0.01 ± 0.005	0.81	↓	0.037	0.176
	C18:1	0.19 ± 0.04	0.14 ± 0.06	0.77	↓	0.002	0.048
	C18:2	0.06 ± 0.02	0.04 ± 0.02	0.66	↓	2.8×10^{-4}	0.015
	C0	37.26 ± 6.11	41.23 ± 6.00	1.11	↑	0.022	0.138
Phospholipids	lysoPC a C18:0	24.71 ± 6.45	20.01 ± 6.61	0.81	↓	0.005	0.078
	PC aa C28:1	2.85 ± 0.84	2.43 ± 0.95	0.85	↓	0.007	0.085
	PC aa C36:2	203.53 ± 51.70	173.58 ± 42.35	0.85	↓	0.012	0.104
	PC aa C38:0	3.04 ± 1.00	2.44 ± 1.58	0.8	↓	0.024	0.139
	PC aa C40:2	0.29 ± 0.11	0.22 ± 0.12	0.76	↓	0.043	0.185
	PC ae C36:3	6.23 ± 1.31	4.94 ± 2.11	0.79	↓	0.036	0.176
	PC ae C38:6	6.95 ± 2.27	5.92 ± 3.08	0.85	↓	0.046	0.195
	PC ae C40:1	1.38 ± 0.42	1.14 ± 0.60	0.82	↓	0.015	0.113
	PC ae C40:4	2.22 ± 0.32	1.77 ± 0.68	0.8	↓	0.015	0.113

	PC ae C42:3	0.74 ± 0.23	0.61 ± 0.29	0.83	↓	0.039	0.176
	PC ae C42:4	0.71 ± 0.25	0.47 ± 0.41	0.67	↓	0.007	0.085
	PC ae C42:5	2.33 ± 0.30	1.67 ± 0.92	0.72	↓	0.001	0.026
	PC ae C44:5	2.1 ± 0.42	1.37 ± 1.22	0.65	↓	0.001	0.026
	PC ae C44:6	1.25 ± 0.31	0.85 ± 0.65	0.68	↓	3.7×10^{-4}	0.015
Sphyngomielyns	SM C24:0	18.29 ± 5.87	14.75 ± 4.30	0.81	↓	0.018	0.113
	SM C24:1	48.12 ± 13.66	41.99 ± 11.09	0.87	↓	0.047	0.195
	SM-OH C24:1	1.25 ± 0.3	0.93 ± 0.49	0.74	↓	0.014	0.113

Fold change, metabolite concentration after RHRT divided by baseline concentration; Cit, citrulline; Orn, ornithine; Pro, proline; Phe, phenylalanine; Val, valine; alpha-AAA, alpha-amino adipic acid; Trp, tryptophan; Cn:z, acylcarnitine, n = number of carbons, z = number of unsaturations; lysoPC Cn:z, lysophosphatidylcholine; PC Cn:z, phosphatidylcholine; SM Cn:z, sphingomyelins; SM OH Cn:z, hydroxylated sphingomyelins. In bold are metabolites with q-values < 0.05. ↓, down-regulated; ↑, up-regulated.

RHRT-induced modulation of metabolic pathways

To explore the systemic biochemical impact of RHRT, all metabolites showing significant post-treatment changes were subjected to metabolic pathway enrichment analysis. Over Representation Analysis (ORA) identified polyamine biosynthesis, the urea cycle, and arginine/proline metabolism as the pathways most strongly influenced by RHRT **(Figure 2a)**.

Serum concentrations of polyamines—including putrescine, spermidine, and spermine—were notably reduced after RHRT, indicating a downregulation of this pathway **(Figure 2b)**. Ornithine, which links the polyamine pathway to the urea cycle, decreased by 12.3% following treatment ($p = 0.02$, $q = 0.113$). While arginine levels remained largely unchanged, citrulline concentrations dropped sharply by 33% ($p = 9 \times 10^{-6}$, $q = 0.001$), with this decline closely correlating with the decrease in ornithine ($r = 0.72$, $p = 0.0005$). Glutamine, another precursor, did not show significant variation, suggesting the effect was pathway-specific. Similarly, proline levels, another ornithine-derived amino acid, fell by 19.2% compared with baseline ($p = 5.3 \times 10^{-3}$, $q = 0.078$).

These findings suggest that RHRT significantly perturbs amino acid metabolism, particularly affecting intermediates linked to polyamine synthesis and the urea cycle, reflecting a systemic host metabolic response to the treatment.

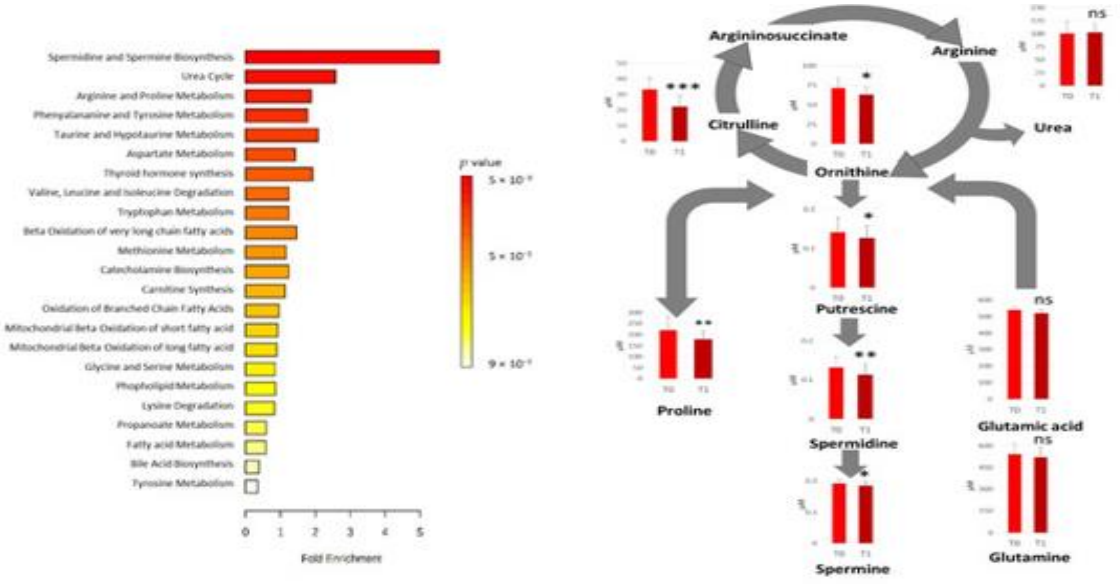

a) b)

Figure 2. Over Representation Analysis plot from enrichment analysis. Bars represent matched pathways coloured according to their significance values, with gradations from yellow (low significance) to red (high significance) (a). Metabolic pathways altered as effect of RHRT and relative metabolites concentrations prior- (T0) and post-RHRT (T1) in 19 malignant pleural Metabolic pathways altered as effect of RHRT and relative metabolites concentrations prior- (T0) and post-R

Dose-dependent effects of RHRT on serum metabolites

Among the metabolite classes, amino acids were the most affected by RHRT, with 14 out of 36 measured amino acids and derivatives showing significant post-treatment alterations. In contrast, the reference group treated with palliative local radiotherapy (LRT) at 21 Gy in 3 fractions displayed minimal metabolomic changes. Only citrulline exhibited a minor decrease (<10%; p = 0.04, q = 0.72) in the LRT cohort. Comparison of mean fold changes for amino acids across the two treatment groups highlighted the more pronounced effect of RHRT, with mean absolute variations of 11.8% (range: 0.44–31.76%) versus 4.0% (range: 0.26–11.8%) observed for LRT-treated patients. These findings underscore the dose-dependent impact of hemithoracic radiotherapy on systemic amino acid metabolism.

Association between RHRT-induced metabolic changes and clinical outcome

The median overall survival (OS) of the RHRT-treated cohort was 24 months (95% CI: 17–43 months), and at the time of metabolomics analysis, all patients had succumbed to MPM. Conventional clinical variables, including age, tumor stage, and performance status, did not correlate with OS. In contrast, post-RHRT changes in serum metabolite levels showed a strong association with survival. Partial least squares (PLS) regression revealed that alterations in specific metabolites explained approximately 60% of the interpatient variability in OS **(Figure 3a)**. Key contributors identified via the loading plot **(Figure 3b)** and Pearson correlation analysis included asymmetric dimethyl-arginine (ADMA), threonine, symmetric dimethyl-arginine (SDMA), putrescine, serine, asparagine, and the acyl-carnitines C2, C10:1, C16:2, and C18:1, with their serum changes positively correlated with longer survival **(Figure 3c)**.

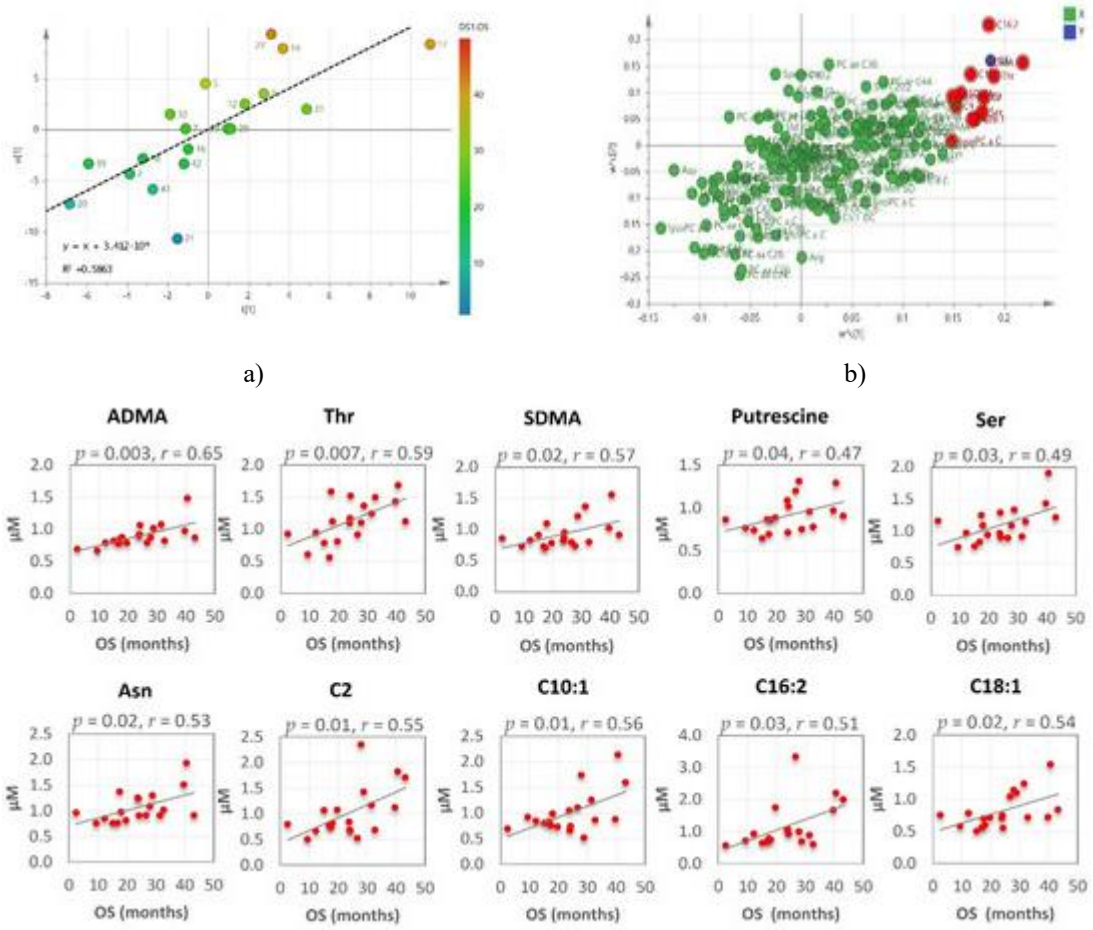

Figure 3. Association of RHRT-Induced Metabolite Changes with Overall Survival

(a) Partial least squares (PLS) score plot of the first two latent variables (t_1 and u_1) illustrating the relationship between serum metabolite fold changes (X block) and overall survival (OS, Y block) for each patient. Points are colored along a gradient from blue to red, indicating increasing OS values.

(b) PLS loading plot showing each metabolite as a point, plotted according to its coefficient on LV1 versus LV2. Metabolites positioned in the top right or bottom left quadrants, corresponding to the highest positive or negative coefficients, exhibit the strongest correlations with OS.
(c) Fold changes of the metabolites most strongly associated with OS, as determined by Pearson correlation analysis.

Stratification of the cohort by OS quartiles revealed a clear trend in metabolite changes: patients with the shortest survival (OS < 16.9 months, Q1) had mean metabolite fold changes of 0.77 ± 0.07 (range: 0.64–0.90), while those with intermediate survival (16.9–28.8 months, IQ) showed fold changes of 1.01 ± 0.14 (range: 0.81–1.26), and patients with the longest survival (OS > 28.8 months, Q4) exhibited fold changes of 1.23 ± 0.17 (range: 0.98–1.47). Notably, analysis restricted to amino acids revealed that long-surviving patients (OS 16.9–43.2 months) experienced, on average, 22% greater metabolic variation than short-surviving patients (OS < 16.9 months) **(Figure 4)**.

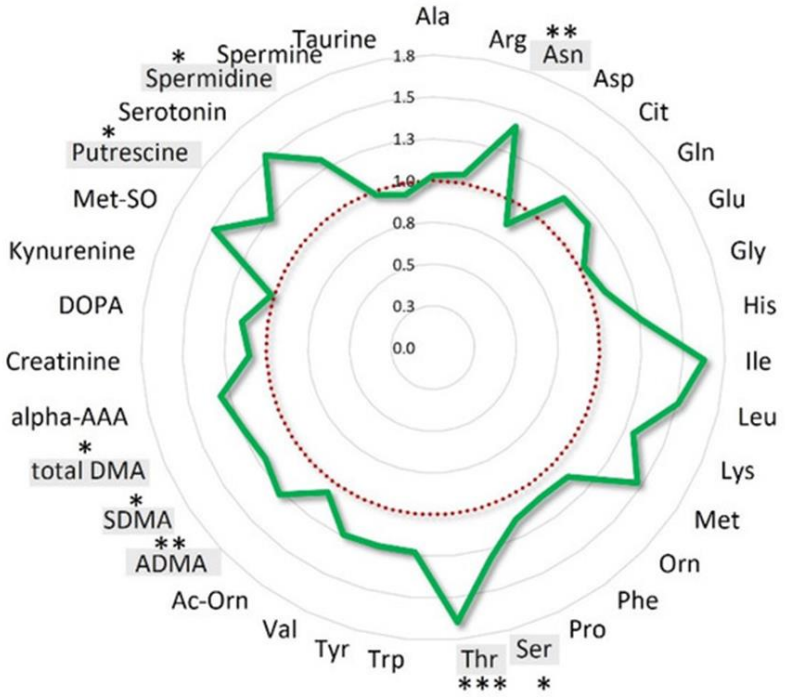

Figure 4. Amino acids mean overall variations of long survival patients normalized to those of short survival patients. Long survival patients belong to IQ (interquartile) and Q4 OS groups; short survival patients belong to the Q1 OS group. Amino acids statistically significant ($p < 0.05$) are highlighted in grey *** $p < 0.001$; ** $p < 0.01$, * $p < 0.05$.

Exposure of tumor and surrounding normal tissues to ionizing radiation triggers a cascade of complex biological responses that extend beyond DNA damage, disrupting tumor metabolism and altering systemic host biochemistry [24].

In this study, we demonstrated that radical hemithoracic radiotherapy (RHRT) induces substantial changes in the serum metabolome of MPM patients, affecting numerous biochemical pathways as a consequence of its action on both tumor and normal tissues. Overall, RHRT led to a marked decrease in most metabolites, a pattern also observed in other cancer types and radiotherapy regimens, suggesting that such systemic metabolite depletion may represent a general feature of the host's metabolic response to irradiation [18, 20–23, 25]. Among the few metabolites that increased post-RHRT were the branched-chain amino acids (BCAAs) valine and leucine. These molecules are key players in protein metabolism, energy production, and various biosynthetic pathways, all of which are typically upregulated in tumor cells [26, 27]. Tumor-driven BCAA catabolism has been linked to systemic depletion of these amino acids [27–29]; thus, the observed post-RHRT rise in valine and leucine may reflect a reduced tumor demand, a phenomenon similarly reported in breast cancer patients where serum BCAAs returned toward normal levels after radiotherapy [17].

Phenylalanine, another essential amino acid, also increased following RHRT. This amino acid is known to rise under inflammatory conditions [30, 31] and correlates with immune activation markers such as neopterin and 8-isoprostane [32, 33]. Radiation is a recognized inducer of oxidative stress, which can trigger acute inflammatory responses [34, 35], and mounting evidence indicates that radiotherapy can also stimulate the immune system [36–39]. The elevation of phenylalanine post-RHRT may, therefore, reflect these immune-modulatory effects.

RHRT was also found to markedly affect lipid metabolism, particularly choline-containing phospholipids including phosphatidylcholines (PC), lysophosphatidylcholines (lysoPC), and sphingomyelins (SM), which showed a significant drop in serum concentration. This decrease likely reflects heightened phospholipid membrane turnover due to radiation-induced tissue damage. Such lipid alterations have been reported in other metabolomics studies following radiotherapy [18, 19, 22, 40] and are thought to be a general effect of irradiation. Beyond their structural role in membranes, phospholipids serve as signaling molecules involved in pathways such as apoptosis [41–43]; therefore, their downregulation may contribute to disrupting tumor signaling and complement the cytotoxic effect of RHRT [44].

Acyl-carnitines were also affected, reflecting changes in fatty acid transport and mitochondrial β-oxidation, critical for energy production. In our cohort, the combination of increased carnitine precursor levels and decreased acyl-carnitines suggests a disruption in their synthesis, potentially due to limited availability of free fatty acids or acetyl-CoA, which may be diverted to support phospholipid replenishment.

While RHRT broadly affected lipid metabolism, enrichment analysis highlighted amino acid-related pathways—specifically, polyamine biosynthesis, the urea cycle, and arginine and proline metabolism—all interconnected via arginine. Arginine, produced primarily in the kidney, plays roles in the urea cycle and other essential pathways such as nitric oxide synthesis [45]. Citrulline, the main endogenous precursor of arginine, was the most strongly reduced metabolite post-RHRT. Citrulline is primarily synthesized in the small intestine from glutamine and ornithine but can also be recycled from nitric oxide production in other tissues [46]. The observed citrulline depletion may reflect reduced intestinal biosynthesis as a collateral effect of high-dose RHRT partially affecting surrounding organs. Citrulline is a recognized biomarker of intestinal dysfunction, with decreases reported in inflammatory bowel disease, chemotherapy, and radiotherapy [14, 47–52]. Despite this drop, arginine levels remained stable, suggesting that systemic mechanisms preserve arginine availability at the expense of citrulline.

The impact of RHRT extended beyond arginine metabolism to the broader amino acid pool, likely due to the high radiation dose. In contrast, patients receiving lower palliative doses of local radiotherapy (LRT) showed minimal metabolic changes, with only a slight decrease in citrulline, indicating dose-dependent effects. Interestingly, citrulline also exhibits antioxidant properties as a radical scavenger [53, 54], suggesting that some depletion in both RHRT and LRT patients may result from its oxidation by reactive oxygen species generated during radiotherapy.

Alpha-aminoadipic acid, released from radiolysis of protein lysine residues [55, 56], was elevated post-RHRT, while taurine, a sulfur-containing amino acid with antioxidant activity, was depleted, likely reflecting increased tissue uptake to counteract radiation-induced oxidative stress [57–61].

Ornithine, another amino acid in the arginine metabolism pathway, also showed significant depletion following RHRT. Its decrease was strongly correlated with citrulline, consistent with its role as a citrulline precursor alongside glutamine [46].

Ornithine can also be synthesized from proline [62], which was significantly reduced following RHRT, indicating that radiation may affect multiple pathways of ornithine biosynthesis. The reduction in ornithine could have important biological implications, as it serves as a precursor for the polyamines putrescine, spermidine, and spermine. These cationic amino acid derivatives are critical regulators of cell proliferation [63], and pharmacological inhibition of their synthesis has been shown to suppress tumor growth in MPM xenograft models [64]. In the context of this study, the observed downregulation of polyamines—likely resulting from decreased ornithine availability—could reflect a potential inhibitory effect on tumor growth, which may contribute to improved disease control in MPM patients.

Collectively, these metabolomic alterations appear to represent a systemic host response not only to counteract radiation-induced stress but also to indirectly modulate tumor progression. Consistent with this notion, the magnitude of the individual metabolic response to RHRT was associated with clinical outcomes. Specifically, changes in amino acids and acyl-carnitine metabolites—including ADMA, threonine, SDMA, putrescine, serine, asparagine, and acyl-carnitines C2, C10:1, C16:2, and C18:1—were positively correlated with overall survival. Patients exhibiting medium-to-long survival showed greater increases in these metabolites post-RHRT,

suggesting that a more robust metabolic adaptation to therapy may confer a survival advantage. Extending this observation to the entire amino acid metabolic network, it appears that long-surviving patients mount a highly dynamic metabolic response, potentially reflecting greater biochemical resilience and metabolic reserves that allow them to better cope with radiation-induced stress while harnessing the therapeutic effects of RHRT.

It should be noted that the relatively small sample size of this study limits the generalizability of these findings. Larger, longitudinal studies are necessary to validate these systemic metabolomic signatures and establish their clinical utility. Future investigations should incorporate time-series sampling throughout radiotherapy and follow-up to distinguish between acute and long-term metabolic effects of RHRT, thereby identifying the most robust prognostic biomarkers. Expanding the metabolomic analysis to additional biological matrices, such as urine, would also provide a more comprehensive understanding of the systemic metabolic response to RHRT.

Materials and Methods

Patient cohort

This metabolomics investigation included 34 patients with histologically confirmed MPM, enrolled between 2014 and 2018 at the Centro di Riferimento Oncologico of Aviano, Italy. All participants had undergone nonradical surgery followed by systemic chemotherapy and were subsequently referred for radiotherapy. Patients were enrolled within a randomized phase III trial comparing the overall survival benefit of RHRT versus standard palliative local radiotherapy (LRT). The study cohort was divided into a test group (n = 19) receiving RHRT and a reference group (n = 15) treated with palliative LRT. RHRT was delivered curatively via intensity-modulated radiation therapy (IMRT) to the entire hemithorax, from the lung apex to the upper abdomen, at a total dose of 50 Gy in 25 fractions, ensuring that 95% of the planned target volume (PTV) received at least 95% of the prescribed dose. Tumor regions with high fluorodeoxyglucose uptake received simultaneous integrated boosts of 60 Gy. In the reference group, LRT was administered at 21 Gy in three fractions targeted to the thoracotomy scar. All patients had preserved pulmonary function and normal baseline renal, hepatic, and hematologic parameters. The study was conducted in accordance with the Declaration of Helsinki and approved by the Ethics Committee of Centro di Riferimento Oncologico di Aviano (Clinical Trial ID: CRO-2013–38). Written informed consent was obtained from all participants.

Sample collection

Peripheral blood samples (5 mL) were collected after overnight fasting at baseline and at the completion of RHRT or LRT. Blood was allowed to clot at room temperature for 30 minutes, followed by centrifugation at 2100 rpm for 15 minutes at room temperature. Serum was aliquoted and stored at −80 °C until metabolomic analysis.

Study design

This investigation aimed to characterize the systemic metabolomic changes induced by radical hemithoracic radiotherapy (RHRT) in 19 patients with malignant pleural mesothelioma (MPM). Serum samples were collected at two time points: prior to the initiation of RHRT (baseline, T0) and after completion of the full 50 Gy/25 fractions regimen (T1). Statistical analyses, including univariate and multivariate approaches, were applied to identify significant alterations in metabolite concentrations. To discern which changes were specifically attributable to RHRT rather than general radiotherapy effects, comparisons were made with a reference cohort of patients treated with palliative local radiotherapy (LRT).

Targeted serum metabolomics profiling

Targeted metabolomic profiling was conducted using the Biocrates Absolute-IDQ P180 platform (Life Science AG, Innsbruck, Austria), which quantifies 188 metabolites across multiple biochemical classes: 21 amino acids, 19 biogenic amines and polyamines, 40 acylcarnitines, 15 lysophosphatidylcholines, 77 phosphatidylcholines, 15 sphingolipids, and one hexose.

Serum samples (10 µL) were thawed and transferred to 96-well plates preloaded with isotopically labeled internal standards. After nitrogen drying, amino acids were derivatized with 5% phenyl isothiocyanate (PTC), followed by a second drying step. Metabolites were extracted using 500 µL of 5 mM ammonium acetate in methanol, filtered, and diluted with MS-compatible solvent for analysis.

Quantification was performed using a Thermo Fisher Ultimate 3000 LC system coupled to a 4000 QTRAP mass spectrometer (AB Sciex, Framingham, MA, USA). FIA-MS/MS was employed for acylcarnitines, lipids, and hexoses, while LC-MS/MS analyzed PTC-derivatized amino acids and biogenic amines on a ZORBAX SB column (100 × 2.1 mm, Agilent). The triple quadrupole operated in MRM, precursor ion, and neutral loss scanning modes, in both positive and negative ionization. Analyst 1.6.1 software was used to integrate MS signals, and calibration curves enabled absolute quantification. Quality control samples at low, medium, and high concentrations ensured analytical reliability. Metabolites below the limit of detection were excluded.

Data processing and statistical analysis

Raw metabolite data were log-transformed and autoscaled prior to analysis. PCA was applied to detect potential outliers and examine overall variance patterns. Supervised OPLS-DA models were constructed to differentiate T0 versus T1 profiles, and model robustness was validated using LOOCV, permutation tests, R^2, and Q^2 metrics. CV-ANOVA was applied to assess model reliability. Metabolites contributing significantly to group separation were identified using VIP scores (>1) and paired t-tests, with FDR adjustment by the Benjamini–Hochberg method ($q < 0.05$).

Metabolites meeting these criteria were further examined through Metabolite Set Enrichment Analysis to identify pathways most affected by RHRT. Mapping to HMDB, PubChem, SMPDB, and KEGG databases enabled classification according to SMPDB pathway libraries, and ORA plots highlighted the most significantly altered pathways.

Finally, associations between metabolite fold-changes (T1/T0) and overall survival (OS) were assessed via PLS regression. Latent variables representing linear combinations of metabolite changes were used to predict OS, with model performance evaluated using R^2, LOOCV, and permutation testing. Metabolites most influential for OS prediction were identified from loading plots ($w*c\,[1] > 0.15$ or < -0.15). Analyses were conducted using SIMCA v14.1, GraphPad Prism 7, and MetaboAnalyst v4.0 [65].

Conclusion

This exploratory study highlights the potential value of integrating metabolomics into the clinical assessment of patients with malignant pleural mesothelioma (MPM). Our findings suggest that systemic metabolic profiling can provide mechanistic insights into the interpatient variability in overall survival following RHRT, as well as identify patients with metabolic phenotypes indicative of heightened vulnerability. With further validation, metabolomics could serve as a robust tool for stratifying patients, guiding clinical decision-making, and identifying those unlikely to derive substantial benefit from RHRT, thereby supporting the development of more tailored, individualized therapeutic strategies.

Acknowledgments: None

Conflict of Interest: None

Financial Support: None

Ethics Statement: None

References

1. Noonan CW. Environmental asbestos exposure and risk of mesothelioma. Ann Transl Med. 2017;5(11):234.
2. Musk AW, Olsen N, Alfonso H, Reid A, Mina R, Franklin P, et al. Predicting survival in malignant mesothelioma. Eur Respir J. 2011;38(6):1420–4.
3. Fahrner R, Ochsenbein A, Schmid RA, Carboni GL. Long term survival after trimodal therapy in malignant pleural mesothelioma. Swiss Med Wkly. 2012; 142(4344):w13686-.
4. Hasegawa S, Okada M, Tanaka F, Yamanaka T, Soejima T, Kamikonya N, et al. Trimodality strategy for treating malignant pleural mesothelioma: Feasibility study... Int J Clin Oncol. 2016;21(3):523–30.
5. Rosenzweig KE. Malignant pleural mesothelioma: Adjuvant therapy with radiation therapy. Ann Transl Med. 2017;5(11):242.

6. Foroudi F, Smith JG, Putt F, Wada M. High-dose palliative radiotherapy for malignant pleural mesothelioma. J Med Imaging Radiat Oncol. 2017;61(6):797–803.
7. Parisi E, Romeo A, Sarnelli A, Ghigi G, Bellia SR, Neri E, et al. High dose irradiation after pleurectomy/decortication or biopsy for pleural mesothelioma treatment. Cancer Radiother. 2017;21(8):766–73.
8. Minatel E, Trovo M, Bearz A, Maso MD, Baresic T, Drigo A, et al. Radical radiation therapy after lung-sparing surgery for malignant pleural mesothelioma. Int J Radiat Oncol Biol Phys. 2015;93(3):606–13.
9. Rosenzweig KE, Zauderer MG, Laser B, Krug LM, Yorke E, Sima CS, et al. Pleural IMRT for malignant pleural mesothelioma. Int J Radiat Oncol Biol Phys. 2012;83(4):1278–83.
10. Clish CB. Metabolomics: An emerging but powerful tool for precision medicine. Cold Spring Harb Mol Case Stud. 2015;1(1):a000588.
11. Corona G, Rizzolio F, Giordano A, Toffoli G. Pharmaco-metabolomics... J Cell Physiol. 2012;227(7):2827–31.
12. Wishart DS. Metabolomics for investigating physiological and pathophysiological processes. Physiol Rev. 2019;99(4):1819–75.
13. Debik J, Euceda LR, Lundgren S, von der Lippe Gythfeldt H, Garred Ø, Borgen E, et al. Serum and tissue metabolomics in breast cancer. J Proteome Res. 2019;18(9):3649–60.
14. Miolo G, Di Gregorio E, Saorin A, Lombardi D, Scalone S, Buonadonna A, et al. Serum metabolomics in metastatic soft tissue sarcoma. Cancers. 2020;12(7):1983.
15. Vignoli A, Muraro E, Miolo G, Tenori L, Turano P, Di Gregorio E, et al. ER status effects on metabolomics in HER2+ breast cancer. Cancers. 2020;12(2):314.
16. Xu PP, Xiong J, Cheng S, Zhao X, Wang CF, Cai G, et al. Phase II study of MEP/Pega + RT in NK/T lymphoma. EBioMedicine. 2017;25:41–9.
17. Arenas M, Rodríguez E, García-Heredia A, Fernández-Arroyo S, Sabater S, Robaina R, et al. Metabolite normalization after radiotherapy. PLoS One. 2018;13(11):e0207474.
18. Jelonek K, Krzywon A, Jablonska P, Slominska EM, Smolenski RT, Polanska J, et al. Serum metabolome in head and neck cancer after RT. Metabolites. 2020;10(3):60.
19. Jelonek K, Pietrowska M, Ros M, Zagdanski A, Suchwalko A, Polanska J, et al. Radiation-induced lipidome changes. Int J Mol Sci. 2014;15(4):6609–24.
20. Laiakis EC, Mak TD, Anizan S, Amundson SA, Barker CA, Wolden SL, et al. Metabolomic radiation signature in urine. Radiat Res. 2014;181(4):350–61.
21. Mörén L, Wibom C, Bergström P, Johansson M, Antti H, Bergenheim AT. Serum metabolome after RT in gliomas. Radiat Oncol. 2016;11(1):51.
22. Nalbantoglu S, Abu-Asab M, Suy S, Collins S, Amri H. Metabolomics biosignatures of prostate cancer after RT. OMICS. 2019;23(5):214–23.
23. Ng SSW, Jang GH, Kurland IJ, Qiu Y, Guha C, Dawson LA. Plasma metabolomics in liver cancer after SBRT. EBioMedicine. 2020;59:102973.
24. Bentzen SM. Preventing or reducing late side effects of radiation therapy. Nat Rev Cancer. 2006;6(10):702–13.
25. Wojakowska A, Zebrowska A, Skowronek A, Rutkowski T, Polanski K, Widlak P, et al. Serum vs exosome metabolomics following RT in HNC. J Pers Med. 2020;10(4):229.
26. Ananieva EA, Wilkinson AC. Branched-chain amino acid metabolism in cancer. Curr Opin Clin Nutr Metab Care. 2018;21(1):64–70.
27. Thewes V, Simon R, Hlevnjak M, Schlotter M, Schroeter P, Schmidt K, et al. BCAT1 in antiestrogen-resistant and ER-negative breast cancer. Oncogene. 2017;36(26):4124–34.
28. Mayers JR, Torrence ME, Danai LV, Papagiannakopoulos T, Davidson SM, Bauer MR, et al. Tissue of origin dictates BCAA metabolism. Science. 2016;353(6306):1161–5.
29. Tönjes M, Barbus S, Park YJ, Wang W, Schlotter M, Lindroth AM, et al. BCAT1 drives proliferation in IDH1-wt gliomas. Nat Med. 2013;19(7):901–8.
30. Geisler S, Gostner JM, Becker K, Ueberall F, Fuchs D. Immune activation increases phenylalanine/tyrosine ratio. Pteridines. 2013;24(1):27–31.
31. Murr C, Grammer TB, Meinitzer A, Kleber ME, März W, Fuchs D. Higher phe/tyr ratios in cardiovascular disease. J Amino Acids. 2014;2014:ID 783730.

32. Neurauter G, Grahmann AV, Klieber M, Zeimet A, Ledochowski M, Sperner-Unterweger B, et al. Serum phenylalanine in ovarian cancer and immune activation. Cancer Lett. 2008;272(1):141–7.
33. Ploder M, Neurauter G, Spittler A, Schroecksnadel K, Roth E, Fuchs D. Serum phenylalanine in patients post trauma and with sepsis correlate to neopterin concentrations. Amino Acids. 2008;35(2):303–7.
34. Jelonek K, Pietrowska M, Widlak P. Systemic effects of ionizing radiation at the proteome and metabolome levels in the blood of cancer patients treated with radiotherapy: the influence of inflammation and radiation toxicity. Int J Radiat Biol. 2017;93(6):683–96.
35. McKelvey KJ, Hudson AL, Back M, Eade T, Diakos CI. Radiation, inflammation and the immune response in cancer. Mamm Genome. 2018;29(11–12):843–65.
36. Deloch L, Derer A, Hartmann J, Frey B, Fietkau R, Gaipl US. Modern radiotherapy concepts and the impact of radiation on immune activation. Front Oncol. 2016;6(6):141.
37. Di Maggio FM, Minafra L, Forte GI, Cammarata FP, Lio D, Messa C, et al. Portrait of inflammatory response to ionizing radiation treatment. J Inflamm. 2015;12(1):14.
38. Huang J, Li JJ. Cell repopulation, rewiring metabolism, and immune regulation in cancer radiotherapy. Radiat Med Prot. 2020;1(1):24–30.
39. Muraro E, Furlan C, Avanzo M, Martorelli D, Comaro E, Rizzo A, et al. Local high-dose radiotherapy induces systemic immunomodulating effects of potential therapeutic relevance in oligometastatic breast cancer. Front Immunol. 2017;8(8):1476.
40. Boguszewicz Ł, Bieleń A, Mrochem-Kwarciak J, Skorupa A, Ciszek M, Heyda A, et al. NMR-based metabolomics in real-time monitoring of treatment-induced toxicity and cachexia in head and neck cancer: a method for early detection of high-risk patients. Metabolomics. 2019;15(8):110.
41. Bartke N, Hannun YA. Bioactive sphingolipids: metabolism and function. J Lipid Res. 2009;50(Suppl):S91–6.
42. Eyster KM. The membrane and lipids as integral participants in signal transduction: lipid signal transduction for the non-lipid biochemist. Adv Physiol Educ. 2007;31(1):5–16.
43. Wright MM, Howe AG, Zaremberg V. Cell membranes and apoptosis: role of cardiolipin, phosphatidylcholine, and anticancer lipid analogues. Biochem Cell Biol. 2004;82(1):18–26.
44. Verheij M, van Blitterswijk WJ, Bartelink H. Radiation-induced apoptosis: the ceramide-SAPK signaling pathway and clinical aspects. Acta Oncol. 1998;37(7–8):575–81.
45. Wu G, Morris SM. Arginine metabolism: nitric oxide and beyond. Biochem J. 1998;336(1):1–17.
46. Curis E, Nicolis I, Moinard C, Osowska S, Zerrouk N, Bénazeth S, et al. Almost all about citrulline in mammals. Amino Acids. 2005;29(3):177–205.
47. Crenn P, Messing B, Cynober L. Citrulline as a biomarker of intestinal failure due to enterocyte mass reduction. Clin Nutr. 2008;27(3):328–39.
48. Blijlevens NMA, Lutgens LCHW, Schattenberg AVMB, Donnelly JP. Citrulline: a potentially simple quantitative marker of intestinal epithelial damage following myeloablative therapy. Bone Marrow Transplant. 2004;34(3):193–6.
49. Ouaknine Krief J, Helly de Tauriers P, Dumenil C, Neveux N, Dumoulin J, Giraud V, et al. Role of antibiotic use, plasma citrulline and blood microbiome in advanced non-small cell lung cancer patients treated with nivolumab. J Immunother Cancer. 2019;7(1):176.
50. Bachmayr-Heyda A, Aust S, Auer K, Meier SM, Schmetterer KG, Dekan S, et al. Integrative systemic and local metabolomics with impact on survival in high-grade serous ovarian cancer. Clin Cancer Res. 2017;23(8):2081–92.
51. Lutgens LCHW, Deutz NEP, Gueulette J, Cleutjens JPM, Berger MPF, Wouters BG, et al. Citrulline: a physiologic marker enabling quantitation and monitoring of epithelial radiation-induced small bowel damage. Int J Radiat Oncol Biol Phys. 2003;57(4):1067–74.
52. Onal C, Kotek A, Unal B, Arslan G, Yavuz A, Topkan E, et al. Plasma citrulline levels predict intestinal toxicity in patients treated with pelvic radiotherapy. Acta Oncol. 2011;50(8):1167–74.
53. Akashi K, Miyake C, Yokota A. Citrulline, a novel compatible solute in drought-tolerant wild watermelon leaves, is an efficient hydroxyl radical scavenger. FEBS Lett. 2001;508(3):438–42.
54. Ginguay A, Regazzetti A, Laprevote O, Moinard C, De Bandt J-P, Cynober L, et al. Citrulline prevents age-related LTP decline in old rats. Sci Rep. 2019;9(1):20138.

55. Requena JR, Chao C-C, Levine RL, Stadtman ER. Glutamic and aminoadipic semialdehydes are the main carbonyl products of metal-catalyzed oxidation of proteins. Proc Natl Acad Sci USA. 2001;98(1):69–74.
56. Sell DR, Strauch CM, Shen W, Monnier VM. 2-Aminoadipic acid is a marker of protein carbonyl oxidation in the aging human skin: effects of diabetes, renal failure and sepsis. Biochem J. 2007;404(3):269–77.
57. Das J, Sil PC. Taurine ameliorates alloxan-induced diabetic renal injury, oxidative stress-related signaling pathways and apoptosis in rats. Amino Acids. 2012;43(4):1509–23.
58. Jong CJ, Azuma J, Schaffer S. Mechanism underlying the antioxidant activity of taurine: prevention of mitochondrial oxidant production. Amino Acids. 2012;42(6):2223–32.
59. Sevin G, Ozsarlak-Sozer G, Keles D, Gokce G, Reel B, Ozgur HH, et al. Taurine inhibits increased MMP-2 expression in a model of oxidative stress induced by glutathione depletion in rabbit heart. Eur J Pharmacol. 2013;706(1–3):98–106.
60. Tabassum H, Rehman H, Banerjee BD, Raisuddin S, Parvez S. Attenuation of tamoxifen-induced hepatotoxicity by taurine in mice. Clin Chim Acta. 2006;370(1–2):129–36.
61. Gao Y, Li X, Gao J, Zhang Z, Feng Y, Nie J, et al. Metabolomic analysis of radiation-induced lung injury in rats: the potential radioprotective role of taurine. Dose Response. 2019;17(4):1–11.
62. Marini JC. Interrelationships between glutamine and citrulline metabolism. Curr Opin Clin Nutr Metab Care. 2016;19(1):62–6.
63. Casero RA, Murray Stewart T, Pegg AE. Polyamine metabolism and cancer: treatments, challenges and opportunities. Nat Rev Cancer. 2018;18(11):681–95.
64. Lam S-K, Yan S, Xu S, Ho JC-M. Targeting polyamine as a novel therapy in xenograft models of malignant pleural mesothelioma. Lung Cancer. 2020;148(1):138–48.
65. Chong J, Wishart DS, Xia J. Using MetaboAnalyst 4.0 for comprehensive and integrative metabolomics data analysis. Curr Protoc Bioinformatics. 2019;68(1):e86.